Theoretical Study on Photophysical and Photochemical Properties of a Merocyanine Dye

Essam Hammam*,† and Ahmed M. El-Nahas*,‡

Chemistry Department, Faculty of Science, Tanta University, Tanta 31527, Egypt, and Chemistry Department, Faculty of Science, El-Menoufia University, Shebin El-Kom, Egypt

Received: December 4, 1997; In Final Form: April 29, 1998

The photophysical and photochemical properties of the merocyanine dye 1-methyl-2-(4-hydroxystyryl)-pyridinium betaine (M) have been studied in aqueous solution at the PM3-SCRF (SCRF = self-consistent reaction field) level of theory. The trans isomer is more stable than the cis one by 6 kcal/mol, and the energy gap decreases upon protonation to 2.4 kcal/mol. Protonation on nitrogen is energetically unfavorable and costs at least 31 kcal/mol more energy than protonation on oxygen. The acidity of the O-protonated form (MH^+) soars up on excitation as inferred from the decrease in the proton affinity values. Potential energy surfaces (PES) for the ground and lowest excited states for the O-protonated (MH^+) and unprotonated (M) forms of the dye have been constructed to explore the deactivation pathways of the excited states. Upon excitation the protonated form adopts the quinonoid geometry of the central single bond, and the trans ⇌ cis photoisomerization goes through a minimum, referred to as the phantom state, of 90° twisted molecular architecture located on the potential energy surface of its first excited singlet state. For the unprotonated form (M), the cis → trans isomerization is a downhill process of a quite negligible energy barrier, surmountable thermally at room temperature. The photochemical/protolytic cycle $M_{trans} \rightleftharpoons MH^+_{trans} \rightleftharpoons MH^+_{cis} \rightleftharpoons M_{cis} \rightarrow M_{trans}$ could be utilized in the storage of information and its subsequent carrier retrieval. The optical transitions are *xy*-plane polarized $\pi-\pi^*$ transitions and are expected at 372 nm (experiment, 364 nm) and 428 nm (experiment, 426 nm) for MH^+ and M, respectively, in aqueous medium. Within the framework of the SCRF model, the unprotonated form (M) exhibits a slight positive solvatochromism. The hydrogen bond donor ability of the solvent is likely the key factor behind the experimentally observed negative solvatochromism.

I. Introduction

Merocyanines are a class of π-conjugated chromophores that can be represented schematically by the general formula D−R−A, where D is the donor, A is the acceptor, and R is the conjugation path.[1] The electronic structure of these compounds can be represented as a combination of benzenoid and quinonoid structures. Although the neutral polyenic resonance form (quinonoid) dominates in molecules with weak donor and acceptor substituents or in solvents having low dielectric constants, the ionic form (benzenoid) is favored in molecules with strong donor and acceptor substituents or in high dielectric constant solvents. The extent to which one of these structures dominates the ground state can lead to different solvatochromic behavior, as reported by Brooker and Daehne.[2]

Due to their extreme solvatochromic properties, merocyanine dyes of stilbazolium betaines have been found to be of more interest among other merocyanines.[3] For some dyes, a reverse solvatochromic behavior has been reported by molecular orbital calculations.[4−6] Merocyanine dyes have been extensively studied experimentally due to their applications. They are used as electrochromic compounds for their membrane potentials and high voltage sensitivity.[7] The photoisomerization of some merocyanine molecules has potential applications in generating erasable photomemory systems.[8] Other merocyanines are used for solar energy conversion as thin films or monolayers on glass substrates.[9] The benzenoid resonance structure of the merocyanine dye is a stilbene-like structure and could suggest the possibility of cis/trans photoisomerization.[10] It has been reported[10,11a,i] that solutions of merocyanine dyes M are photochemically more stable and these findings are suggestive of a photoreaction of the protonated form, MH^+. The quantum yields Φ_{t-c} and Φ_{c-t} are of equal order of magnitude, the sum being close to unity.[10] The photoinduced cis/trans isomerism of organic molecules about unsaturated linkages is a phenomenon that has been recognized for some time and has been the subject of many reported studies.[11] Indeed, in at least two cases, this type of photochemical reaction can be truly said to be a part of everyone's daily life. The trans/cis isomerism of urocanic acid in the epidermis has been suggested as a mechanism by which part of harmful energy of the ultraviolet radiation is dissipated by the body,[12] and the isomerism of rhodopsin, which is the vicinal pigment in the desk membranes of vertebrates' rod photoreceptors, is well-documented as being the primary act in the detection of light by the retina.[13]

In this paper we are theoretically reporting on the structure, cis/trans photoisomerization, and the solvatochromism of 1-methyl-2-(4-hydroxystyryl)pyridinium betaine (M) in an attempt to correlate the calculated results with the available experimental findings.[3c,10]

II. Methods of Calculations

All calculations have been performed with the VAMP program.[14] The geometries of different conformations of merocyanine dye (M) and its protonated form MH^+ are fully optimized using the PM3[15] Hamiltonian in the gas phase as well as in the solvent media. The PRECISE option is used, as

† Tanta University. E-mail: e.hammam@usa-net.
‡ El-Menoufia University.

10.1021/jp9804244 CCC: $15.00 © 1998 American Chemical Society
Published on Web 11/05/1998

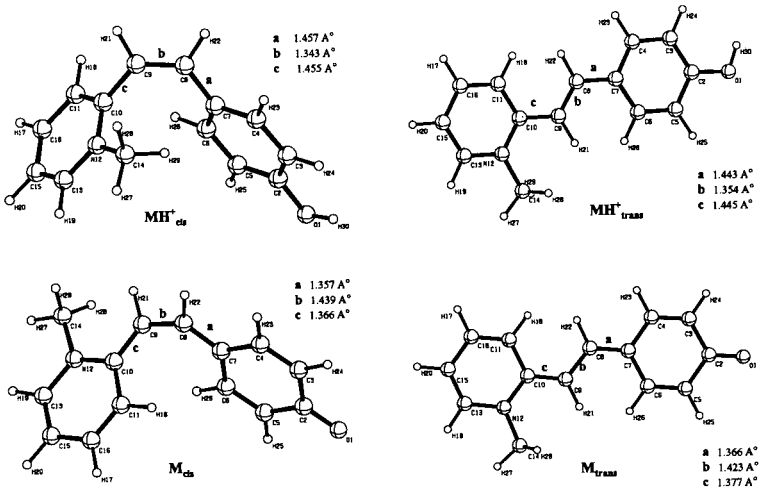

Figure 1. Optimized structures for O-protonated (MH^+) and unprotonated (M) merocyanine dye at PM3 in aqueous solution.

recommended,[16] for augmenting the convergence criteria for the consistent field iterations and for geometry optimization. All geometries are fully optimized without symmetry constraint (i.e. at C_1 symmetry).

For embracing the effect of solvent the numerical self-consistent reaction field (SCRF) formalism[4,17a] extented to excited states—as implemented in the semiempirical package Vamp[14]—has been employed. In this model, following the Tomasi suggestion,[17b] the polarization of a homogeneous infinite dielectric medium—characterized by its dielectric constant (ϵ)—is reduced to the creation of a system of virtual charges on the surface of a numerically derived cavity containing the solute. The free energy of solvation ($\Delta G^{\text{solv}}_{\text{tot.}}$) is taken as the sum of the electrostatic interaction of solute with the induced reaction filed ($\Delta G^{\text{solv}}_{\text{estat}}$), the dispersion interaction of solute with the dielectric continuum ($\Delta G^{\text{solv}}_{\text{disp}}$), and the free cavity energy ($\Delta G^{\text{solv}}_{\text{cav}}$).

$$\Delta G^{\text{solv}}_{\text{tot.}} = \Delta G^{\text{solv}}_{\text{estat}} + \Delta G^{\text{solv}}_{\text{disp}} + \Delta G^{\text{solv}}_{\text{cav}}$$

The arbitrarily shaped solvent cavity[4] is represented by a polyhedron with a finite set of faces s_i located approximately at the van der Waals surface of the molecule and carries a charge density proportional to the gradient of the molecular potential (V) at the cavity surface due to the charge distributions of the solute; which is described by multipole expansion. Thus the induced surface charge density $\sigma(r_s)$ can be expressed by

$$\sigma_i(r_s) = -\alpha(\partial V/\partial n)_s$$

Here, $(\partial V/\partial n)_s$ is the gradient of the numerically calculated molecular potential—described by the NAO/PC model[17c]—at position r_s in the direction of the normal n to the surface element directed toward the dielectric. The factor α describes the dielectric relaxation of solvent in an electric filed and could be represented by a variety of functions[4] that differ in how the time evolution of the relaxation process is included in the model. Thus a finite set of surface charges q_i is determined by

$$q_i = \sigma(s_i)\,\Delta S_i$$

where ΔS_i is the area of surface element i.

Within the framework of the SCRF model, the impact of the solvent on the solute is taken into account self-consistently and treated quantum mechanically by introducing an additional one-electron term to the Fock operator $\hat{f}^\circ$ of solute in vacuo:

$$\hat{f}(j) = \hat{f}^\circ(j) - \sum_i \frac{q_i}{r_{ij}}$$

with r_{ij} being the distance between electron j and surface element s_i. Within the semiempirical NDDO formalism the one-center term of the Fock matrix in the basis of atomic orbitals is given by

$$F_{u^\alpha v^\beta} = F^\circ_{u^\alpha v^\beta} - \delta_{\alpha\beta}\sum_i q_i(u^\alpha v^\beta | s^i s^i)$$

To calculate the energetic properties of an excited state, its energy of solvation must be calculated in a reaction field that is induced by the charge distribution of this state. The first-order correlated density matrix is used to compute the electrostatic component of the total energy of solvation and determine the polarizability tensor that is used in the calculation of the dispersion contribution.[4] While this corresponds to that of full relaxation of the solvent molecules, the calculation of the optical transitions requires the division of solvent polarization into orientational (inertial) and electronic (fast) relaxations. In fast Frank—Condon electronic transition, complete relaxation of the electronic polarization of the solvent is assumed, whereas the orientational polarization—which is equal for all states in the CI expansion—corresponds still to that induced by the ground-state charge distribution of solute.[4] For additional mathematical details, ref 4 should be consulted.

To calculate the electronic spectra, we have used configuration interaction (CI) expansion limiting the CI to single and pair double excitations (PECI = 8).[4] The electronic excitations are vertical in nature.[18] Absorption ($S_0 \rightarrow S_1$) spectra have been calculated at the MNDO[19] level using the PM3 optimized geometries in solvent media. At this theoretical level a good correlation between theory and experiment is obtained.[20]

III. Results and Discussion

IIIA. Structures and Effect of Solvent. Depending on the polarity of the medium as well as its pH, the stilbazolium betaine adopts two equilibrium molecular architectures, Figure 1: the polyene-like (quinonoidal) and polymethine-like (benzenoidal) geometries. The change in geometry between these two molecular extremes could be indexed by bond length alternation (BLA)[21] defined as the difference between the average single

TABLE 1: Variation of Bond Length Alternation (BLA) Index, the Wavelength of Maximum Absorption (λ_{max}), the Dipole Moment (μ), and the Solvation Energy (ΔH_{solv}) as a Function of the Medium Polarity and $F(\epsilon)$, for Unprotonated Stilbazolium Betaine (M)

medium	$F(\epsilon)$[a]	BLA[b] (Å)	λ_{max} (nm)	μ[c] (D)	ΔH_{solv} (kcal/mol)
gas phase	0.000	0.064	416.0	9.04	0.0
hexane	0.188	0.060	419.9	9.93 (9.90)	−0.98
CCl_4	0.222	0.059	420.4	10.08 (10.03)	−1.14
ether	0.340	0.057	423.1	10.73 (10.62)	−1.83
chloroform	0.356	0.056	423.6	10.85 (10.72)	−1.95
CH_2Cl_2	0.420	0.054	425.4	11.27 (11.09)	−2. 37
acetone	0.464	0.052	426.9	11.59 (11.36)	−2.70
ethanol	0.470	0.052	427.1	11.63 (11.39)	−2.74
methanol	0.477	0.052	427.4	11.69 (11.44)	−2.79
acetonitrile	0.480	0.052	427.4	11.70 (11.45)	−2.81
DMSO[d]	0.485	0.052	427.4	11.74 (11.48)	−2.85
water	0.490	0.052	427.8	11.79 (11.52)	−2.90

[a] $F(\epsilon) = (\epsilon - 1)/(2\epsilon + 1)$, where ϵ is the static dielectric constant of the medium. [b] The bond length alternation index (BLA) is equal to the difference between the length of bond C_8-C_9 and the average length of the bonds of C_7-C_8 and C_9-C_{10}. [c] Values in parentheses are the dipole moments of the dye (M) upon excitation vertically to the first excited singlet state S_1, the nonequilibrium Franck−Condon state, in different media. [d] DMSO = dimethyl sulfoxide.

and double bond distances in the conjugated pathway of the stilbazolium betaine. The BLAs as a function of solvent dielectric constant are listed in Table 1.

In the gas phase, the unprotonated form of the dye (M) adopts the quinonoidal geometry of the C_s point group of symmetry and the dipole moment of 9.04 D. The charge distribution is mostly localized on both the pyridinium and phenoxy moieties of charge densities of $+0.26e$ and $-0.21e$, respectively. Apart from the increase in the heat of solvation, the BLA index of the initial value of 0.064 Å in the gas phase changes slightly, see Table 1, as the solvent dielectric soars up, indicating that the solvent reaction field is not strong enough to induce appreciable geometric distortion in the conjugation path of the dye. In contrast, the charge distribution is highly affected by the solvent polarity. In aqueous medium, for example, a charge of about of $+0.1e$ is transferred from the pyridinium to the phenoxy moiety, clarifying the increase in the dipole moment by about 3D on its value in the gas phase. About half of the transferred charge resides on the terminal oxygen atom of the latter moiety.

Stereochemically, the merocyanine dye (M) ultimately adopts either the cis or trans molecular architectures; see Figure 1. To shed light on stabilities of these isomers, potential energy surfaces have been constructed by anglewise rotation around the C_8-C_9 bond in a step of 30°. A cursory glance at Figure 2, for S_0, reveals the existence of a minimum at a torsional angle of 180° and a shoulder at 55°. The minimum represents the trans isomer, while the shoulder maps out the twisted cis one which deviates from planarity by coulombic and steric repulsions between the aromatic rings. The coplanar cis isomer could be localized at a torsional angle of 0°. It should be clear that the presence of the $N-CH_3$ group at the ortho position relieves the steric crowding as the twist angle increases from the coplanar cis configuration; see Figure 1. The stability of the trans isomer exceeds that of the nonplanar and planar cis counterparts by 2.0 and 6.0 kcal/mol, respectively.

The basic form of the dye (M) could be protonated on either the N_{12} or O_1 atom; see Figure 1. To resolve the site of protonation on thermochemical backgrounds, the proton affinities (PAs), at temperature (T) defined by the minus of the

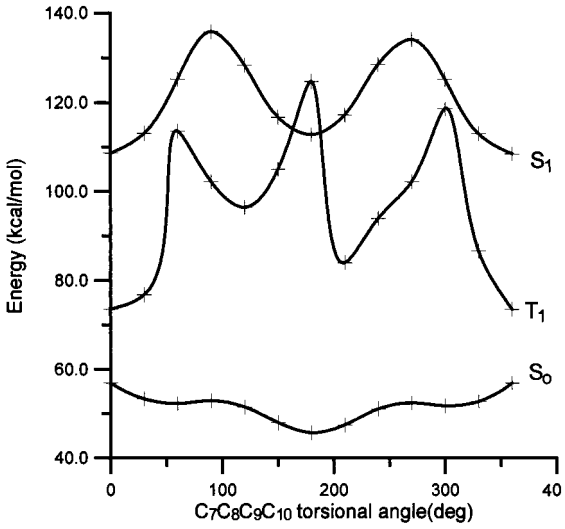

Figure 2. Potential energy surfaces for the ground and lowest excited states for merocyanine dye as a function of the angle of twist at PM3 in aqueous solution.

TABLE 2: Heats of Formation (kcal/mol) and Proton Affinity (PA) for Protonated (MH^+) and Unprotonated (M) Forms of Merocyanine Dye in Aqueous Medium at 25°

	heats of formation kcal/mol			PA (kcal/mol)		
species	S_0	S_1	T_1	S_0	S_1	T_1
M_{trans}	46.18	113.21	79.84	268.67	254.15	255.76
M_{cis}	52.21	108.91	74.42	273.03	249.55	210.88
$MH^+_{trans/O}$	144.71	225.89	191.28			
$MH^+_{cis/O}$	147.09	226.56	239.74			
$MH^+_{trans/N}$	191.40	269.62	222.60			
$MH^+_{cis/N}$	191.40	269.62	222.60			

enthalpy change in the reaction,

$$M + H^+ \rightarrow MH^+, \quad PA(M) = -\Delta H^\circ_T(r)$$

are computed in different electronic states, Table 2, by

$$PA(M) = \Delta H^\circ_{f,T}(H^+) + \Delta H^\circ_{f,T}(M) - \Delta H^\circ_{f,T}(MH^+)$$

where $\Delta H^\circ_{f,T}$ represents the heat of formation at 298 K. For $\Delta H^\circ_{f,298}(H^+)$ the experimental value of 367.2 kcal/mol was used.[22]

In all cases, protonation on the oxygen atom is strongly preferred over that on nitrogen by a minimum of 31 kcal/mol; see Table 2. This finding is consistent with previous studies reported on similar merocyanine dyes.[10,11a,i,23] Upon protonation, the energy gap between the O-protonated trans and planar cis isomers shrinks to 2.4 kcal/mol in aqueous solution. The protonated form has most of its positive charge, ca. 98%, localized on the pyridinum moiety.

Being drawn from the decrease in the values of proton affinities, Table 2, the increase in acidity of the conjugate acid (MH^+) upon excitation could be justified too from the density of charge of the hydroxyl group of its phenolic moiety. For the most stable trans isomer, excitation to S_1, for example, results in decreasing the density of charge on the oxygen atom, O_1, from $-0.21e$, in the ground state, to $-0.15e$. On hydrogen atom, H_{30}, the charge density increases from $+0.22e$, in the ground state, to $+0.24e$. The diminution of the negative charges on both the oxygen and hydrogen atoms facilitates the polarization of the σ bonding pair of electrons toward the former atom, making the ionization of the latter easier.

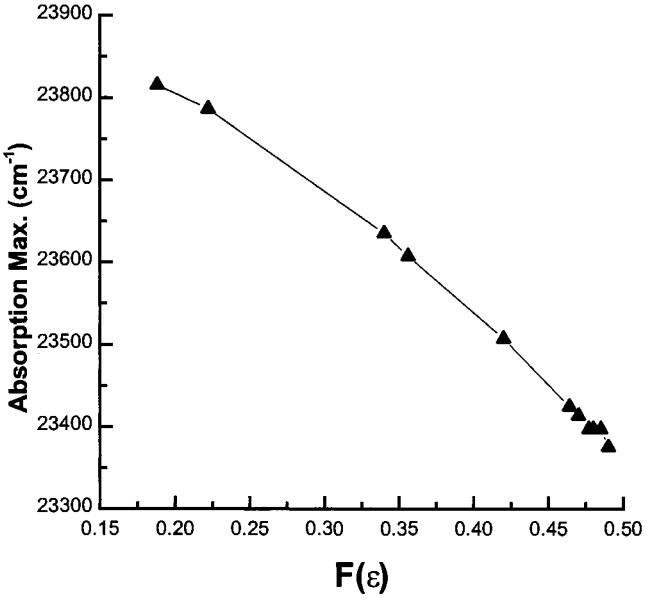

Figure 3. Variation of the calculated wave number of maximum absorption as a function of the dielectric constant of solvent $F(\epsilon)$, where $F(\epsilon) = (\epsilon - 1)/(2\epsilon + 1)$ and ϵ is the static dielectric constant of the solvent.

In aqueous medium, the electronic optical transitions for protonated (MH^+) and unprotonated (M) forms of the dye are expected at 372 nm [24] with oscillator strength 0.89 and 428 nm with oscillator strength 1.18, respectively. These findings agree very well with the experimental values,[23] which are 364 and 426 nm for MH^+ and M, respectively. These electronic transitions are assigned to $\pi-\pi^*$ types of transitions and are polarized in the *xy*-plane with deviations from the *x*-axis by -15 and $-10°$ for MH^+ and M, respectively.

The solvatochromic variation of the optical transition energy of the unprotonated form of stilbazolium betaine (M) as a function of solvent dielectric constant is shown in Figure 3. The molecule exhibits a slight positive solvatochromism. Although this theoretical behavior agrees qualitatively with what has been calculated by Albert et al.[1] on similar merocyanine dyes, particularly before using the experimentally determined cavity radius, unfortunately, it does not go in line with the experimental finding.[3c] Experimentally,[10] it has been found that the long-wavelength absorption maximum exhibits strong negative solvatochromy which has been rationalized qualitatively by assuming that the large ground-state dipole moment of the molecule is reduced by excitation. Bayliss and McRae[25a] have shown that the underlying change in the electronic structure is mainly due to the hydrogen bonding ability of the solvent rather than its bulk polarity, which is the only physical quantity included in the SCRF model used in the present set of calculations.

It should be kept in mind that, in the present continuum model, the cavity is solute specific and solvent invariant. The solvent is merely taken into account by its reaction field, which influences the energy of the solute. Moreover, the representation of hydrogen bonding in the continuum model is, in general, strongly limited.[4] Rauhut et al.[4] tried to overcome the effect of hydrogen bonding in protic solvents empirically by adjusting the atomic van der Waals radii used in the construction of the cavity to reproduce the experimental solvation energies of a set of 30 molecules. Even by doing that, the error is not completely corrected, with the exception of water. Hence, as a clear disadvantage of the present SCRF model is the arbitrary choice of the the van der Waals radii to construct the cavity.

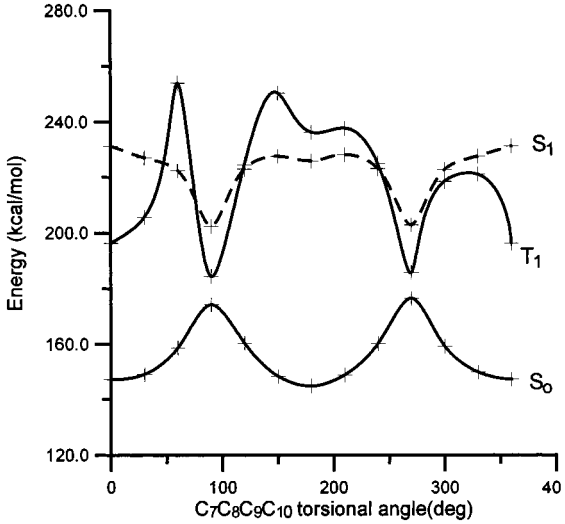

Figure 4. Potential energy surfaces for the ground and lowest excited states for the O-protonated merocyanine dye as a function of the angle of twist at PM3 in aqueous solution.

One might have to resort to a more realistic cavity-based formalism such as the self-consistent isodensity polarized continuum model[25b] (SCI-PCM) which gives rise to a cavity dependent on both the solute and solvent irrespective of the the atomic van der Waals radii.

The excellent matching between experiment and theory in the case of water as a solvent in the present study might indicate that the atomic van der Waals radii used to construct the cavity is so optimized that the hydrogen bonding is taken into account which affects to a large extent the solvatochromic behavior of such merocyanine dye. The decrease in the dipole moment upon excitation—although it is marginal, see Table 1—may be the clue to the negative solvatochromy of the present merocyanine dye as previously suggested.[10]

IIIB. Cis/Trans Photoisomerization. The close resemblance of the molecular architectures of the present merocyanine dye (M) and its conjugate acid (MH^+) to stilbene, 4-stilbazole, and the 4-stalbazolium cation strongly conveys the possibility of trans/cis photoisomerization. As reported by Steiner et al.,[10] the trans forms of the conjugate acid of a similar merocyanine dye photoisomerizes to the cis one, and vice versa, by a singlet mechanism involving the phantom state of 90° twisted configuration as intermediate of a lifetime shorter than 5 ns. As far as the unprotonated form is concerned, the possibility of its trans → cis photoisomerization was ruled out.

To clarify the mechanistic pathway of photoisomerization for the present merocyanine dye (M) at the level of *theory* in light of the previous discussion—with the motivation of good agreement between the calculated and experimentally recorded optical transitions, especially in aqueous medium—the potential energy surfaces (PESs) have been constructed for the dye (M) and its protonated form (MH^+) in different electronic states by anglewise rotation around the C_8-C_9 bond, Figures 2 and 4. As an essential prerequisite for a potential trans/cis photoisomerization is the absence of a sizable energy barrier on the torsional coordinate from trans ⇌ cis in the excited state with localization of most of the excitation energy on the ethylenic double bond.

In the ground state, the trans and cis isomers of the merocyanine dye (M) have BLA indices with values 0.052 and 0.078 Å, respectively, which reflect the quinonoid molecular architecture of the dye. In this geometry, either isomer of the dye has a central single bond. Upon excitation to S_1, the dye

adopts the benzenoid geometry of a central ethylenic bridge as inferred from the reversal in the values of BLA to −0.064 and −0.077 Å for the trans and cis isomers, respectively. In this case, either isomer has to surmount an energy barrier of 25 kcal/mol on the torsional coordinate to isomerize to the other form; see Figure 2. The presence of this high activation energy might favor a high-fluorescence quantum yield. But as the PES of T_1 intercepts with that of S_1 at torsional coordinate very close to 180°, the $S_1 \rightarrow T_1$ intersystem crossing (ISC) will be a highly probable radiationless channel for the decay of S_1 with the result of lowering the fluorescence quantum yield dramatically for the trans isomer.[10]

Upon pondering the PES of the ground state of the dye (M), see Figure 2, it becomes quite clear that the cis → trans isomerization is a downhill process of a quite negligible energy barrier, of 0.63 kcal/mol, thermally surmountable at room temperature. More important is that when the dye adopts the 90° twisted configuration, °perp, in the ground state, its cis → trans photoisomerization becomes a downhill process of no energy barrier tracing the sequence: °cis ⇌ °perp → ^{1}perp → (^{1}trans + ^{3}twist) → °trans, where ^{3}twist is a twisted triplet of torsional angle 120°; see Figure 2. It must be borne in mind that the first step in this sequence is thermally dependent, while the second one is photodriven with a probable $S_1 \rightarrow T_1$ ISC to ^{3}twist which decays to the ground-state surface from which it finally ends up in the trans ground state; see Figure 2. The downhill nature of the ^{1}perp → ^{1}trans twisting process may contribute in rendering the cis isomer nonfluorescent; i.e., $\varphi_F = 0$.

On being protonated, the dye adopts the benzenoidal molecular geometry of a ethylenic bridge as concluded from the BLA of values −0.089 and −0.113 Å, for the trans and cis isomers, respectively. Thus in the ground state, either form of the dye cannot isomerize thermally to the other one owing to a sizable barrier of 27 kcal/mol on the torsional coordinate from trans ⇌ cis located at 90°; see Figure 4. In the first excited singlet state most of the excitation energy is localized on the ethylenic bridge based on the increase in the BLA by +0.1 and +0.12 Å on its value in the ground state for the trans and cis isomers, respectively. This implies that the geometrical photoisomerization for these isomers proceeds by fast twisting around a single bond from the trans (cis) excited singlet, ^{1}trans (^{1}cis), to a minimum which maps out the "phantom singlet" with a perpendicular equilibrium geometry, ^{1}perp; see Figure 4. From ^{1}perp the molecule decays by internal conversion to the ground-state surface, °perp, from which by fast relaxation it ends up in the cis and trans ground states with partitioning ratios a and $1 - a$, respectively. The exact localization of ^{1}perp with that of °perp on a torsional coordinate of 90° is a computational challenge. The partitioning ratio is expected to be more or less 1:1 for comparable probability for deactivation of °perp to either cis or trans ground states of nearly matched energies. The lower energy barrier, of 1.6 kcal/mol for the twisting process from ^{1}trans → ^{1}perp, see Figure 4, retards to some extent of time the ^{1}trans from decaying once it is formed to the phantom singlet. This may be the clue to the fluorescent character of the trans isomer, and the lower value[10] of its φ_F, as compared to the nonfluorescent cis one of the downhill ^{1}cis → ^{1}perp twisting process. In this geometrical photoisomerization it is theoretically expected that the lifetime (τ) of the excited state is 2.33 ns, as deduced[26] from

$$\tau/\mathrm{s} = 1.500/f\nu^2$$

where f is the oscillator strength of value 1.18 and ν is the wave number of the optical transition for the trans isomer of value 23 364 cm^{-1}; see above. This time regime of the excited state is consistent with the result of the laser flash experiment,[10] on a similar merocyanine dye, that showed trans → cis conversion to be complete within 5 ns. The interception of the PES for T_1 with that for S_1 does not rule out the possibility of the ISC to a "phantom triplet", ^{3}perp, which decays nonradiatively to the ultimate cis and trans ground states. From the application point of view, the photochemical and protolytic properties of the present merocyanine, as has emerged from the previous discussion, could be utilized judiciously in designing[10,27] a photodriven proton pump of one direction functionality as sketched in Figure 5.

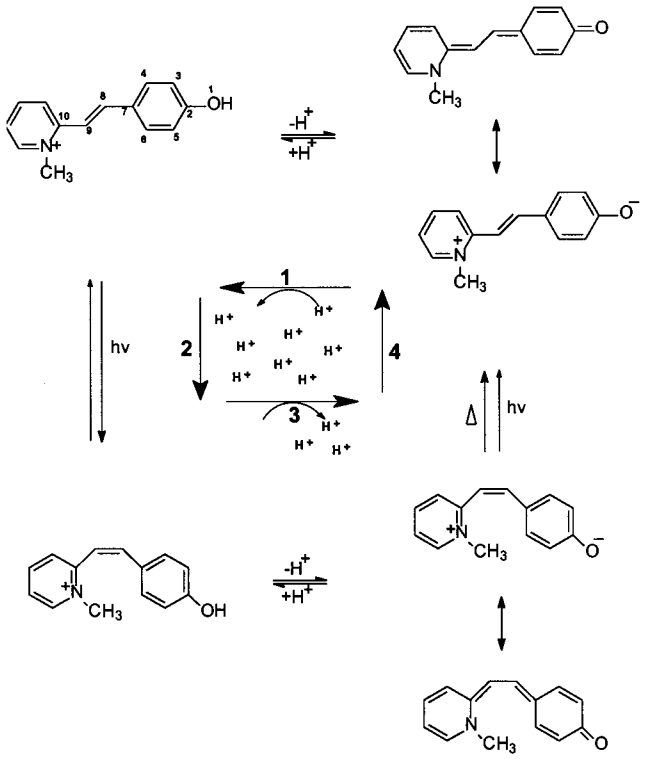

Figure 5. Photochemical/protolytic cycle for merocyanine dye as a model for a photodriven proton pump. By the reaction sequence 1, 2, 3, 4, 1, ..., protons are pumped from inside to outside in one direction due to irreversibility of step 4.

Acknowledgment. The authors wish to thank Dr. P. Gedeck of Computer Chemie Centrum, University of Erlangen, Germany, for many stimulating discussions on the SCRF model.

References and Notes

(1) Albert, D. I.; Marks, T. J.; Ratner, M. A. *J. Phys. Chem.* **1996**, *100*, 9714.

(2) (a) Radeglia, R.; Daehne, S. *J. Mol. Struct.* **1970**, *5*, 399. (b) Daehne, S.; Hoffman, K. *Prog. Phys. Org. Chem.* **1990**, *18*, 1. (c) Daehne, S. *Chimica* **1991,** *45*, 288. (d) Brooker, L. G. S.; Keys, G. H.; Sprague, R. H.; Van Dyke, R. H.; Van Zandt, E.; White, F. L. *J. Am. Chem. Soc.* **1951,** *73*, 5326.

(3) (a) Brooker, L. G. S.; Keyes, G. H.; Heseltine, D. W. *J. Am. Chem. Soc.* **1951,** *73*, 5350. (b) Huenig, S.; Rosenthal, O. *Justus Liebigs Ann. Chem.* **1955**, *161*, 592. (c) Abdel-Halim, S. T. *J. Chem. Soc., Faraday Trans.* **1993**, *89*, 55.

(4) Rauhut, G.; Clark, T.; Steinke, T. *J. Am. Chem. Soc.* **1993**, *115*, 9174.

(5) Botrel, A.; Beuze, A.; Jacques, P.; Strub, H. *J. Chem. Soc., Farady Trans. 2* **1984**, *80*, 1235.

(6) Jacques, P. *J. Phys. Chem.* **1986**, *90*, 5535.

(7) (a) Grinwald, A.; Frostig, R. D.; Licke, E.; Hildesheim, R. *Phys. Rev.* **1985**, *8*, 263. (b) Loew, L. M.; Scully, S.; Simpson, L.; Waggoner, A. S. *Nature (London)* **1979**, *281*, 497.

(8) Horie, H.; Hirao, K.; Kenochi, N.; Mita, J. *Makromol. Chem. Rapid Commun.* **1988**, *9*, 267.

(9) Arden, W.; Fromherz, P. *J. Electrochem. Soc.* **1980**, *127*, 372. Inacker, O.; Kuhn, H.; Mobius, D.; Debuch, G. Z. *J. Phys. Chem.* **1976**, *101*, 337.

(10) Steiner, U.; Abdel-Kader, M. H.; Fischer, P.; Kramer, H. E. A. *J. Am. Chem. Soc*. **1978**, *100*, 3190.

(11) (a) Abdel-Kader, M.; Steiner, U. *J. Chem. Educ.* **1983**, *60*, 160. (b) Vedamuthu, M.; Singh, S.; Onganger, Y.; Essire; D. R.; Yin, M.; Quitevis, E. L.; Robinson, G. W. *J. Phys. Chem.* **1996**, *100*, 11907. (c) Orlandi, G.; Palmieri, P.; Poggi, G. *J. Am. Chem. Soc.* **1979**, *101*, 3492. (d) Askin, J. S.; Anares, L.; Pedersen, S.; Ewail, V. H. *J. Phys. Chem.* **1996**, *100*, 11920. (e) Bartocci, G.; Mazzucato, U.; Masetti, F. *J. Phys. Chem.* **1980**, *84*, 847. (f) Bartocci, G.; Masetti, F.; Mazzucato, U.; Spalletti, A.; Baraldi, I.; Momicchioli, F. *J. Phys. Chem.* **1987**, *91*, 4733. (g) Mazzucat, U. *Gazz. Chim. Ital*. **1987**, *117*, 661. (h) Bartocci, G.; Masetti, F.; Mazzucato, U.; Spalletti, A. *J. Chem. Soc., Farady Trans. 2* **1988**, *84*, 385. (i) Schulte-Frohlinde, D.; Guesten, H. *Liebigs Ann. Chem.* **1971**, *49*, 749.

(12) Baden, H. P.; Pathake, M. A.; Butler, D. *Nature* **1966**, *210*, 732.

(13) Wald, G. *Science* **1968**, *162*, 230.

(14) Rauhut, G.; Chandrasekhar, J.; Clark, T. University of Erlangen, Germany, **1992**. Vampc 4.55 implemented on PCs by B. Wiedel.

(15) Dewar, M. J. S.; Zoebisch, E. G.; Healy, E. F.; Stewart, J. J. P. *J. Am. Chem. Soc*. **1985**, *107*, 3902.

(16) Boyd, B.; Smith, D. W.; Stewart, J. J. P.; Wimmer, E. *J. Comput. Chem.* **1988**, *9*, 387.

(17) (a) Gedeck, P.; Schneider, S. *J. Photochem. Photobiol. A: Chem.* **1997**, *105*, 165. (b) Miertus, S.; Tomasi, J. *Chem. Phys.* **1982**, *65*, 239. (c) Rauhut, G.; Clark, T. *J. Comput. Chem*. **1993**, *14*, 503.

(18) (a) Nakano, H.; Tsuneda, T.; Hashimoto, T.; Hirao, K. *J. Chem. Phys.* **1996**, *104*, 2312. (b) Hashimoto, T., Nakano, H.; Hirao, K. *J. Chem. Phys*. **1996**, *104*, 6244.

(19) Dewar, M. J. S.; Thiel, W. *J. Am. Chem. Soc.* **1977**, *99*, 4899.

(20) El-Nahas, A. M.; Hammam, E.; Ebeid, E. *J. Comput. Chem.* **1998**, *19*, 585.

(21) Marder, S. R.; Beratan, D. N.; Cheng, L.-T. *Science* **1991**, *103*, 252.

(22) Stull, D. R., Prophet, H., Eds.; *JANAF Thermochemical Tables*; National Bureau of Standards, National Standard Reference Data Series NSRDS-NBS 37 (U.S. Government Printing Office: Washington, D.C., 1971.

(23) Abdel-Halim, S. T.; Awad, M. K. *J. Phys. Chem.* **1993**, *97*, 3160.

(24) Calculated by using the Conductor-like Screening Model (COSMO) implemented in MOPAC93 with keywords EPS and NSPA set to 78.4 and 60, respectively.

(25) (a) Bayliss, N. G.; McRae, E. G. *J. Am. Chem. Soc.* **1954**, *58*, 718. (b) Foresman, J. B.; Keith, T. A.; Frisch, M. J.; Murcko, M. *J. Phys. Chem.* **1996**, *100*, 16096.

(26) Milton, M.; Jaffe, H. H. *Symmetry, Orbital, and Spectra (S.O.S.)*; Wiley: New York, 1971.

(27) Schulten, K.; Tavan, P. *Nature* (*London*) **1978**, *272*, 85.